Optimization of Tether Length in Nonglycosidically Linked Bivalent Ligands That Target Sites 2 and 1 of a *Shiga*-like Toxin

Pavel I. Kitov,[†] Hiroki Shimizu,[‡] Steven W. Homans,[‡] and David R. Bundle*,[†]

Contribution from the Chemistry Department, University of Alberta,
Edmonton, Canada T6G 2G2 and School of Biochemistry and Molecular Biology,
University of Leeds, Leeds LS2 9JT, United Kingdom

Received February 7, 2002 ; E-mail: Dave.Bundle@ualberta.ca

Abstract: A series of bivalent ligands for a *Shiga*-like toxin have been synthesized, their experimentally determined inhibitory activities were compared with a simplified thermodynamic model, and computer simulations were used to predict the optimal tether length in bivalent ligands. The design of the inhibitors exploits the proximity of the C-2′ hydroxyl groups of two P^k-trisaccharides when bound to two different, neighboring carbohydrate recognizing binding sites located on the surface of *Shiga*-like toxin. NMR studies of the complex between the toxin and bivalent ligands show that site 2 and site 1 of a single B subunit are simultaneously occupied by a tethered P^k-trisaccharide dimer. A simplified thermodynamic treatment provides the intrinsic affinities and binding energies for the intermolecular and intramolecular association events and permits the deconvolution of the contributions to the relative binding energies for the set of bivalent ligands. Conformational analysis based on MD simulations for bivalent galabioside dimers containing different tethers demonstrated that the calculated local concentrations of the pendant ligand at the second binding site correlate with the experimentally determined relative affinity values of the respective bivalent ligands, thereby providing a predictive method to optimize tether length.

Introduction

Intervention in the recognition of mammalian cell surface oligosaccharides by secreted or surface bound lectins of pathogenic organisms is a potentially attractive therapeutic strategy to combat bacterial adherence[1] or microbial toxin binding and entry into specific cells.[2] However, the realization of this objective is frustrated by the low intrinsic affinity for acceptance of a polar oligosaccharide in to what is nearly always a hydrophilic, shallow depression in the protein surface of the lectin. Tight binding is achieved through multivalent binding facilitated by the occurrence of more than one carbohydrate recognition site per lectin subunit, as well as the oligomeric nature of many lectins, and the presence on mammalian cells of very large numbers of glycolipids or glycoproteins that display the relevant oligosaccharide structure. Numerous attempts to emulate Nature's multivalency by creating oligo- or polymeric presentations of oligosaccharides have met with varied success.[3]

Despite the landmark and spectacular example of hepatic lectin binding to terminal galactose residues displayed on multiantennary glycans,[4] for the most part short oligosaccharides displayed randomly on various polymers achieve rather modest gains in avidity, especially when compared to the number of saccharide units attached to the polymer. The limited avidity gains presumably arise because only a small fraction of the available saccharides is able to bind with the lectin. Development of a viable strategy that could reliably make more effective use of every saccharide unit by adjusting the spatial display to match the separation of the lectin sites is a challenging but worthwhile approach, as illustrated by the recent reports of spectacular avidity gains for penta- and decavalent inhibitors that bind to the class of AB_5 bacterial toxins.[5,6] Translation of such tailored multivalency to the recognition of cell surface oligosaccharides by mammalian lectins would have potential for intervention in inflammatory responses[7] and a myriad of other cell−cell interactions that are known to depend on
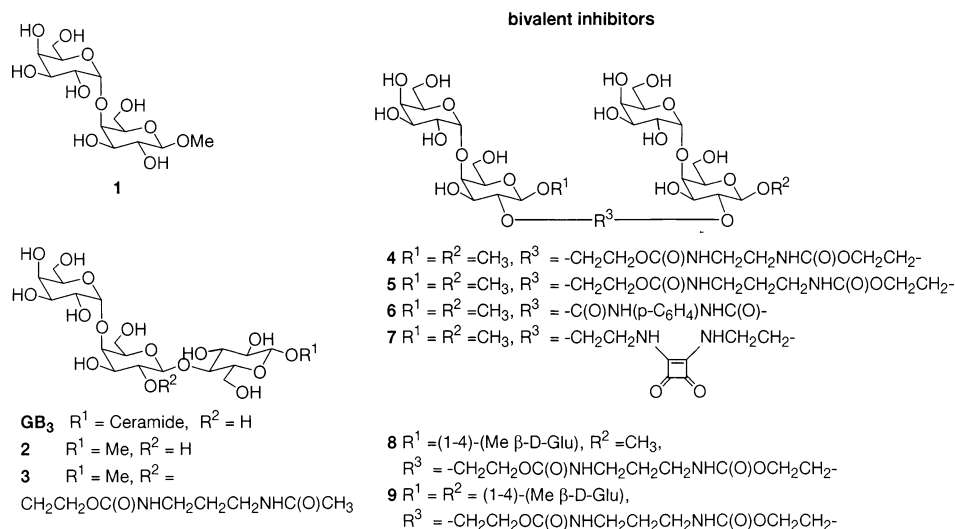
† University of Alberta.
‡ University of Leeds.
(1) Aronson, M.; Medalia, O.; Schori, L.; Mirelman, D.; Sharon, N.; Ofek, I. *J. Infect. Dis.* **1979**, *139*, 329−32.
(2) (a) Karlsson, K.-A.; Milh, M. A.; Ångström, J. In *Molecular Recognition in Host Parasite Interactions*; Korhonen, T. K., Ed.; Plenum Press: New York 1992; pp 115−32. (b) Karlsson, K.-A. *Trends Pharmacol. Sci.* **1991**, *12*, 265−72.
(3) Mammen, M.; Choi, S. K.; Whitesides, G. M. *Angew. Chem., Int. Ed.* **1998**, *37*, 2755−94.

(4) (a) Lee, Y. C.; Townsend, R. R.; Hardy, M. R.; Lonngren, J.; Arnarp, J.; Haraldsson, M.; Lonn, H. *J. Biol. Chem.* **1983**, *258*, 199−202. (b) Lee, R. T.; Lin, P.; Lee, Y. C. *Biochemistry* **1984**, *23*, 4255−61. (c) Lee, R. T.; Lee, Y. C. *Glycoconjugate J.* **2000**, *17*, 543−51.
(5) (a) Kitov, P. I.; Sadowska, J. M.; Mulvey, G.; Armstrong, G. D.; Ling, H.; Pannu, N. S.; Read, R. J.; Bundle, D. R. *Nature* **2000**, *403*, 669−72. (b) Bundle, D. R.; Kitov, P. I.; Read, R. J.; Ling, H.; Armstrong, G. D. Treatment of Bacterial Dysentery. U.S. Patent 5,962,423, Oct 5, 1999. (c) Bundle, D. R.; Kitov, P.; Read, R. J.; Ling, H.; Armstrong, G. Treatment of Bacterial Infections. U.S. Patent 6,310,043, Oct 30, 2001.
(6) (a) Fan, E. K.; Zhang, Z. S.; Minke, W. E.; Hou, Z.; Verlinde, C. L. M. J.; Hol, W. G. J. *J. Am. Chem. Soc.* **2000**, *122*, 2663−64. (b) Merritt, E. A.; Zhang, Z. S.; Pickens, J. C.; Ahn, M.; Hol, W. G. J.; Fan, E. K. *J. Am. Chem. Soc.* **2002**, *124*, 8818−8824. (c) Zhang, Z.; Merritt, E. A.; Ahn, M.; Roach, C.; Hou, Z.; Verlinde, C. L. M. J.; Hol, W. G. J.; Fan, E. *J. Am. Chem. Soc.* **2002**, *124*, 12991−8.
(7) Springer, T. A. *Nature* **1991**, *349*, 196−7.

Scheme 1

bivalent inhibitors

1

HO—OMe

GB₃ R¹ = Ceramide, R² = H
2   R¹ = Me, R² = H
3   R¹ = Me, R² = CH₂CH₂OC(O)NHCH₂CH₂CH₂NHC(O)OCH₃

4 R¹ = R² = CH₃, R³ = -CH₂CH₂OC(O)NHCH₂CH₂NHC(O)OCH₂CH₂-
5 R¹ = R² = CH₃, R³ = -CH₂CH₂OC(O)NHCH₂CH₂CH₂NHC(O)OCH₂CH₂-
6 R¹ = R² = CH₃, R³ = -C(O)NH(p-C₆H₄)NHC(O)-
7 R¹ = R² = CH₃, R³ = -CH₂CH₂NH⎯⎯NHCH₂CH₂-

8 R¹ = (1-4)-(Me β-D-Glu), R² = CH₃,
    R³ = -CH₂CH₂OC(O)NHCH₂CH₂CH₂NHC(O)OCH₂CH₂-
9 R¹ = R² = (1-4)-(Me β-D-Glu),
    R³ = -CH₂CH₂OC(O)NHCH₂CH₂CH₂NHC(O)OCH₂CH₂-

oligosaccharide-based recognition.[8] Here, we report our attempts to develop a predictive procedure for optimizing the spacing of tethered oligosaccharides.

Shiga-like toxins (SLTs) belong to a small but clinically significant family of AB₅ bacterial toxins.[9] They consist of a cytotoxic enzyme A subunit noncovalently linked to a homopentameric cell-adhesion carrier, B₅. The entry of the enzymic A subunit into the host cell relies on adhesion of the B₅ subunit to the cell membrane, an interaction that is highly specific and mediated by Pᵏ-trisaccharide, the carbohydrate constituent of Gb₃ glycolipid, also called CD77.[10] Inhibition of toxin binding to the host-cell surface is an attractive antiadhesive therapy for bacterial infections.[11]

The solved crystal structure[12] of the complex between *Shiga*-like toxin type 1 (SLT-1) and a soluble analogue of Pᵏ-trisaccharide, α-D-Gal(1−4)-β-D-Gal(1−4)-β-D-GlcOR, reveals 15 Pᵏ-trisaccharide binding sites of three distinct types. Although all three types of binding sites recognize the same cell-surface receptor, their relative affinity established by site-directed mutagenesis[13] decreases in the order: site 2 > site 1 > site 3 (the designation of binding sites is according to ref 14 and does not necessarily follow the order of affinity). The intrinsic affinities are very low, and even with the highest affinity, site 2 has an association constant of 500−1000 M⁻¹ for Pᵏ-trisaccharide as determined by microcalorimetry.[15] Site 1 is estimated by NMR to have only 10−15% of the site 2 activity.[16] We have previously demonstrated by mass spectrometry that the equilibrium distribution of ligand bound and unbound SLT-1 B₅ species indicates at least an order of magnitude difference between the two highest binding constants.[17]

A large number of Pᵏ-tri- and disaccharide analogues have been synthesized by us[18] and others,[14] and their activities evaluated. However, no viable univalent lead compound could be identified. It appears that the plurality of the binding modes compromises the chances to create a small molecular weight inhibitor that would be equally efficient for blocking all three possible binding pockets found on the surface of the toxin. On the other hand, the multitude of binding modes provides an opportunity to explore the effect of multivalent interaction with both equivalent and nonequivalent binding sites as a target. The arrangement of all three sites across the surface of the toxin makes it reasonable to predict that tethering of several Pᵏ-trisaccharide units into one cluster will increase the inhibitory activity due to what is commonly referred to as the cluster glycoside effect.[19]
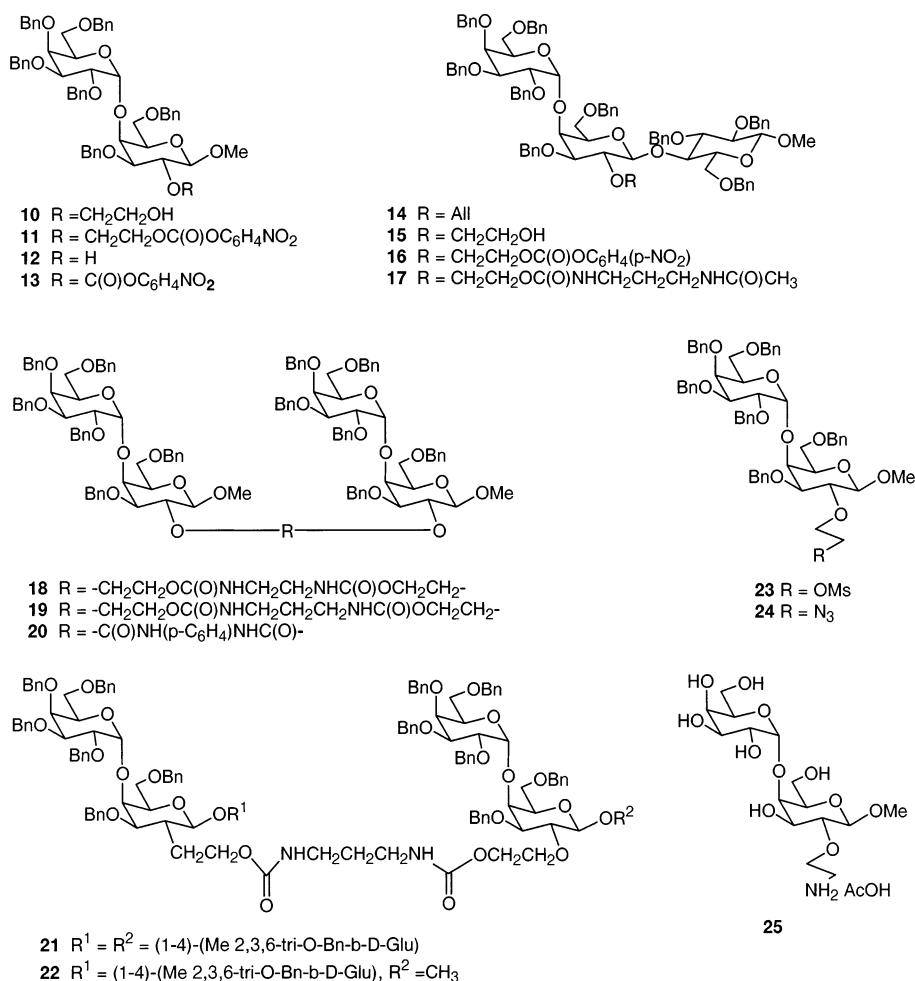
Design of Inhibitors. Examination of the crystal structure suggested an opportunity for bridging two neighboring molecules of the trisaccharide bound to site 1 and site 2, respectively. Despite its participation in water-mediated hydrogen bonding, the hydroxyl group at the C-2 position of the β-Gal moiety is not directly involved in any crucial interactions with the protein in either site 1 or site 2.[18] The distance between the O-2′ atoms of two Pᵏ-trisaccharides bound in site 1 and site 2 is only 11 Å, and the path between the two is not obstructed by any protein residue. Previously, we have demonstrated that alkyl substituents at the O-2′ position of Pᵏ-trisaccharide do not significantly affect binding to SLT-1.[18] Therefore, bridging between those two nonglycosidic hydroxyls presented an attractive alternative to tethering via glycosidic positions, which is more common in the design of multivalent glycoconjugates. For the majority of model dimers, we have chosen a synthetically efficient, carbamate-containing bridge, the length of which can be readily adjusted, and one tether is constructed using a bifunctional squarate derivative. We present here the synthesis of six such dimers **4−9** (Scheme 1) containing di- and trisaccharide units.

Synthesis of SLT-1 Inhibitors. The general assembly strategy for synthesis of bivalent di- and trisaccharide ligands

(8) Varki, A. *Glycobiology* **1993**, *3*, 97−130.
(9) Merritt, E. A.; Hol, W. G. J. *Curr. Opin. Struct. Biol.* **1995**, *5*, 165−71.
(10) Lindberg, A. A.; Brown, J. E.; Stromberg, N.; Westerling-Ryd, M.; Schultz, J. E.; Karlsson, K.-A. *J. Biol. Chem.* **1987**, *262*, 1779−85.
(11) Sharon, N.; Ofek, I. *Glycoconjugate J.* **2000**, *17*, 659−64.
(12) Ling, H.; Boodhoo, A.; Hazes, B.; Cummings, M. D.; Armstrong, G. D.; Brunton, J. L.; Read, R. J. *Biochemistry* **1998**, *37*, 1777−88.
(13) (a) Bast, D. J.; Banerjee, L.; Clark, C.; Read, R. J.; Brunton, J. L. *Mol. Microbiol.* **1999**, *32*, 953−60. (b) Soltyk, A. M.; MacKenzie, C. R.; Wolski, V. M.; Hirama, T.; Kitov, P. I.; Bundle D. R.; Brunton, J. L. *J. Biol. Chem.* **2002**, in press.
(14) Nyholm, P. G.; Magnusson, G.; Zheng, Z.; Norel, R.; Binnington-Boyd, B.; Lingwood, C. A. *Chem. Biol.* **1996**, *3*, 263−75.
(15) St. Hilaire, P. M.; Boyd, M. K.; Toone, E. J. *Biochemistry* **1994**, *33*, 14452−63.
(16) Richardson, J. M.; Evans, P. D.; Homans, S. W.; Donohue-Rolfe, A. *Nat. Struct. Biol.* **1997**, *4*, 190−3.

(17) Kitova, E. N.; Kitov, P. I.; Bundle, D. R.; Klassen, J. S. *Glycobiology* **2001**, *11*, 605−11.
(18) Kitov, P. I.; Bundle, D. R. *J. Chem. Soc., Perkin Trans. 1* **2001**, 838−853.
(19) Lundquist, J. J.; Toone, E. J. *Chem. Rev.* **2002**, *102*, 555−8.

Scheme 2

10 R =CH$_2$CH$_2$OH
11 R = CH$_2$CH$_2$OC(O)OC$_6$H$_4$NO$_2$
12 R = H
13 R = C(O)OC$_6$H$_4$NO$_2$

14 R = All
15 R = CH$_2$CH$_2$OH
16 R = CH$_2$CH$_2$OC(O)OC$_6$H$_4$(p-NO$_2$)
17 R = CH$_2$CH$_2$OC(O)NHCH$_2$CH$_2$CH$_2$NHC(O)CH$_3$

18 R = -CH$_2$CH$_2$OC(O)NHCH$_2$CH$_2$NHC(O)OCH$_2$CH$_2$-
19 R = -CH$_2$CH$_2$OC(O)NHCH$_2$CH$_2$CH$_2$NHC(O)OCH$_2$CH$_2$-
20 R = -C(O)NH(p-C$_6$H$_4$)NHC(O)-

23 R = OMs
24 R = N$_3$

21 R^1 = R^2 = (1-4)-(Me 2,3,6-tri-O-Bn-b-D-Glu)
22 R^1 = (1-4)-(Me 2,3,6-tri-O-Bn-b-D-Glu), R^2 =CH$_3$

25

involves activation of a hydroxyl group of a partially protected oligosaccharide derivative as its *p*-nitrophenyl carbonate, followed by coupling with an amine to form a carbamate linkage. Oxidation of the double bond of the allyl derivative **14**[18] with 4-methylmorpholine *N*-oxide in the presence of OsO$_4$ followed by the cleavage of the resulting diol with NaIO$_4$ and subsequent reduction of the resulting aldehyde with NaBH$_4$ provided alcohol **15** (Scheme 2). Esterification of **10**,[18] **12**,[18] and **15** with *p*-nitrophenyl chloroformate in pyridine gave the corresponding *p*-nitrophenyl carbonates **11**, **13**, and **16**, which served as key building blocks for installation of carbohydrate determinants into the oligomeric inhibitors. Condensation of **11** with ethylenediamine and propylenediamine afforded two homologous bridged disaccharide dimers **18** and **19**. Reaction of **13** with *p*-phenylenediamine provided dimer **20** containing an aromatic bridge. Because of the low nucleophilicity of the aromatic amine, the reaction requires rather forcing conditions: extended time, elevated temperature, and nucleophilic catalysis with DMAP. The symmetric trisaccharide dimer **21** was obtained by the reaction of **16** with propylenediamine, and the mixed di- and trisaccharide dimer **22** was synthesized by the consecutive treatment of propylenediamine with one equiv of **11** then with **16**. Compound **17**, which consists of a trisaccharide attached to the tether fragment, was obtained by coupling of **16** with one equiv of propylenediamine followed by the acetylation of the product with acetic anhydride. Catalytic debenzylation of

17−**22** afforded the target P^k-trisaccharide analogues **3**−**6**, **8**, and **9**.

The synthesis of squaric acid derivative **7** also starts from the common precursor **10**. Mesylation gave compound **23**, which was converted into azide **24** by nucleophilic displacement. Catalytic hydrogenation of the azido functionality accompanied by debenzylation afforded the deprotected amino derivative **25**. Condensation of 2 equiv of **25** with bifunctional squarate gave target digalabioside **7**.

Evaluation of Inhibitory Activity. A competitive solid-phase assay was employed for evaluation of the inhibitory activities of the P^k-trisaccharide tethered dimers **4**−**9** (Figure 1). We have previously reported details of this assay.[18] In brief, the recombinant B$_5$ subunit of SLT-1 was immobilized on the wells of microtiter plates, and then a solution of P^k-trisaccharide/BSA/biotin glycoconjugate was coincubated in the microtiter well in the absence or presence of various concentrations of inhibitor. For each concentration of inhibitor, the assay was performed in triplicate. After 18 h of equilibration, the plate was washed with buffer and the amount of bound biotin was measured by a standard biotin-streptavidin protocol. The results are presented in the Table 1.

NMR Studies of the Complex between the SLT-1 B$_5$ Subunit and Bivalent Ligand 9. To obtain direct structural evidence for the simultaneous binding to two distinct sites, we employed a "SAR-by-NMR" approach[20] to examine the
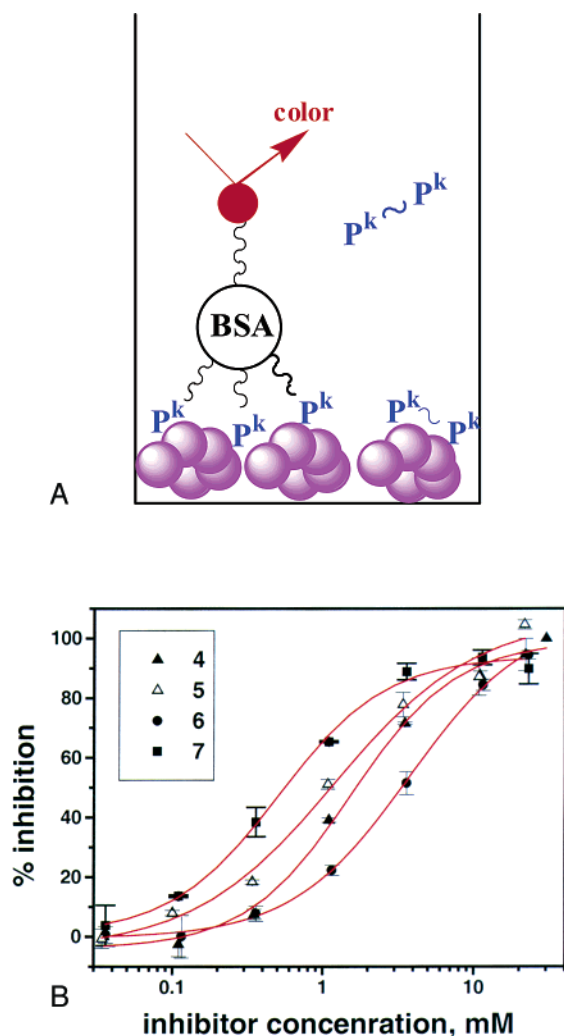
Figure 1. (Panel A) Schematic representation of the competitive ELISA used to measure inhibitor activity. (Panel B) Representative example of binding data. Error bars represent the standard error for triplicates.

Table 1. Activities of Synthetic SLT-1 Inhibitors

compound	number of ligands	$1/IC_{50}$ (M^{-1})	relative activities[a]
1[18]	1	33	1
2[18]	1	4.7×10^2	
3	1	7.1×10^2	
4	2	7.7×10^2	23.3
5	2	1.03×10^3	31.2
6	2	2.5×10^2	7.57
7	2	1.56×10^3	47.3
8	2	3.9×10^3	
9	2	1.8×10^4	

[a] With respect to monovalent galabioside **1**.

interaction of **9** with the uniformly ^{15}N-enriched *Shiga*-like toxin B$_5$ subunit. Shown in Figure 2 are overlaid ^{15}N–^{1}H HSQC spectra of the B$_5$ subunit alone (black contours) and in the presence of a 4-fold molar excess (with respect to monomer B) of **9** (red contours). Substantial chemical shift changes in the complex provide direct evidence for binding of **9** to the protein. By use of ^{15}N and H^N resonance assignments obtained in a previous NMR study of the B subunit homopentamer,[16] these

(20) Shuker, S. B.; Hajduk, P. J.; Meadows, R. P.; Fesik, S. W. *Science* **1996**, *274*, 1531–4.

shift changes can be mapped onto the three-dimensional structure of the protein.[12] It is immediately obvious from these data that the resonances derived from Thr 31, Asp 18, Asp 17, Glu 65, and Lys 53 are shifted in a fashion that reflects those observed in a previous study on the binding of P^k-trisaccharide.[21] In that study, these shift changes were shown to arise from binding at site 2. In the present study, these shift changes are more substantial, because the affinity of **9** is greater than P^k-trisaccharide, resulting in a larger fraction of complexed protein. Additional shifts of comparable magnitude to those mentioned previously can be observed in Figure 2. Shifts of resonances assigned to Thr 19, Thr 21, Glu 28, and Lys 13 are of particular note, since these were not detected previously in the SLT-1B–P^k-trisaccharide complex.[16,21] As the amino acids responsible for these resonances are located in site 1 of the crystal structure, the data taken together suggest that **9** simultaneously occupies sites 1 and 2. In addition to the resonance shifts mentioned thus far, a number of other significant shifts are observed in Figure 2 (e.g., Gly 61). The residues corresponding to these shifts are common to both sites 1 and 2, and hence, we interpret these shifts as arising from the combined effect of simultaneous occupancy of both sites.

One formal alternative interpretation of these data is that **8** simultaneously occupies sites 1 and 2, in two different B subunit molecules. However, in this hypothetical case, the resulting complex would exhibit a large molecular correlation time with significant broadening of resonances in ^{15}N–^{1}H HSQC spectra, which is a characteristic of such large complexes (~75 kDa). Contrary to those expectations, the resonance line widths in the complex of the B subunit with **9** are substantially *smaller* than those for the B$_5$ subunit alone, and hence, we can confidently rule out this alternative interpretation. The basis of this line narrowing is currently under investigation via ^{15}N NMR relaxation time measurements.

Molecular Dynamics Simulations. We constructed the surrogate binding site {1,2} consisting of site 1 and site 2 by modifying the crystal structure of the complex between SLT-1 and P^k-trisaccharide glycoside.[12] Tether elements were added, and the glucose moieties in bound P^k-trisaccharides were replaced by methyl groups. Only side chains of selected amino acids were retained in order to form a bumping surface that limits the conformational space available for the pendant ligand and tether. During simulations, the positions of the former protein atoms were fixed and a harmonic tether of 100 kcal/mol was applied to the disaccharide bound to site 2 (Figure 3). Since relatively high barriers of rotation for single bonds would preclude collection of representative conformational distributions at room temperature in a reasonable period of time, all MD experiments were conducted at a temperature of 1000 K.

Discussion

It has been previously shown that the IC$_{50}$ values in this competitive assay format with a labeled glycoconjugate as the reporter molecule closely approximate the K_D values between the inhibitor of interest and the protein receptor.[22] Indeed, the data for methyl glycosides of galabiose **1** and P^k-trisaccharide

(21) Shimizu, H.; Field, R. A.; Homans, S. W.; Donohue-Rolfe, A. *Biochemistry* **1998**, *37*, 11078–82.
(22) (a) Vorberg, E.; Bundle, D. R. *J. Immunol. Methods* **1990**, *132*, 81–9. (b) Sigurskjold, B. W.; Altman, E.; Bundle, D. R. *Eur. J. Biochem.* **1991**, *197*, 239–46.
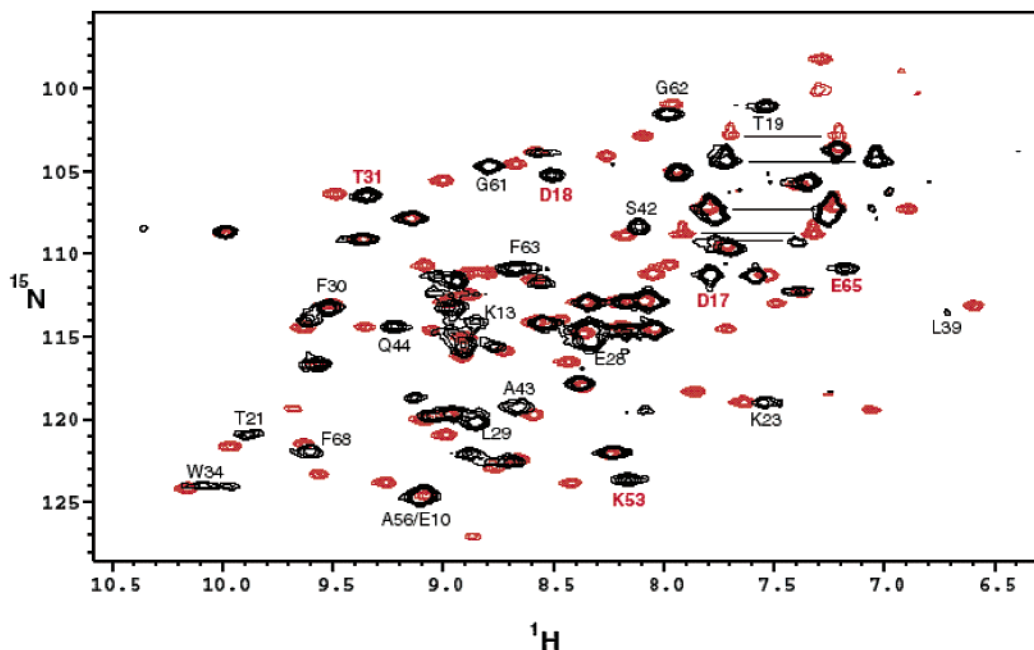
Figure 2. Overlaid $^{15}N-^{1}H$ HSQC spectra of ^{15}N-enriched *Shiga*-like toxin B subunit homopentamer in the absence (black contours) and presence (red contours) of P^k-trisaccharide dimer **9** in 4-fold molar excess over protein monomer. Assignments of key resonances that exhibit shifts between the two spectra are labeled in the usual notation. Assignments shown in red type correspond with those that were observed to shift in a previous study of the B subunit–P^k-trisaccharide complex.[16]
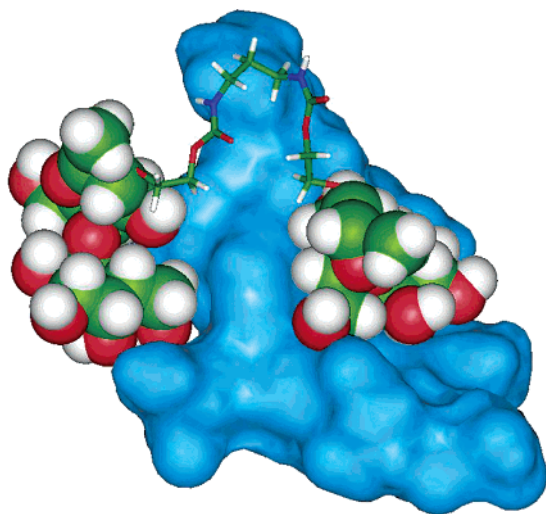

Figure 3. Structure of SLT-1–dimer **5** complex prepared for MD simulation. Bound galabioside (left) in site 2 is constrained by a force of 100 kcal/mol to its crystal structure position. Free movements of tethered pendant galabioside (shown on the right in its original position in site 1) are limited by a bouncing surface formed by side chains of selected amino acids.

2 obtained in our assay are in good agreement with K_D values measured by microcalorimetry.[15] This is a rather fortuitous coincidence due to two mutually compensating effects. Although, generally, IC$_{50}$ values obtained in a competitive assay are systematically higher than the absolute values of K_D, in the case of the interaction of a monovalent ligand with a multivalent receptor, the statistical factor leads to an increase of apparent activity. However, the overriding importance of a solid-phase competitive assay conducted under consistent conditions is the reproducibility of the *relative* values of K_D. These are sufficiently accurate for the comparative purposes discussed here.

When compared with univalent ligands (galabioside **1** and P^k-trisaccharide **2**), bivalent ligands **4–9** show substantially higher activity. The activity of the P^k-trisaccharide **3**, which contains only a fragment of the propylenediamine tether, does not differ significantly from that of unmodified trisaccharide **2**. This indicates that possible nonspecific interactions between the protein surface and structural elements of the tether do not contribute significantly to binding and the affinity of the dimeric analogues results from protein–carbohydrate interactions. In the series of dimeric ligands containing the propylenediamine tether **5**, **8**, and **9**, the activities progressively increase with the number and affinity of the ligands attached to both ends of the tether. Thus, the weakest dimeric ligand is the dimer of P^k-disaccharides **5**, and the strongest is the dimer of P^k-trisaccharides **9**.

Multivalency effects observed for dimers **5**, **8**, and **9** that contain the same propylenediamine-based tether can be interpreted in terms of a simplified thermodynamic model. It was suggested by Jencks[23] that the standard free energy of binding for composite ligands A–B is the sum of $\Delta G°$ values for the individual interactions A and B combined with a contribution by the tether.

$$\Delta G° = \Delta G°_A + \Delta G°_B + \Delta G°_{tether} \qquad (1)$$

In the case of symmetrical dimers, the statistical term $RT \ln 2$ must be introduced in order to account for the effectively double concentration of ligand.

The relationship between the elementary interactions of univalent and bivalent ligands with a composite binding site {1,2} is delineated in Figure 4. This diagram allows a tentative estimate of the individual contributions to the interaction of di- and trisaccharides in binding sites 1 and 2. In conjunction with NMR data for the complex of **9** with the toxin, this balance of

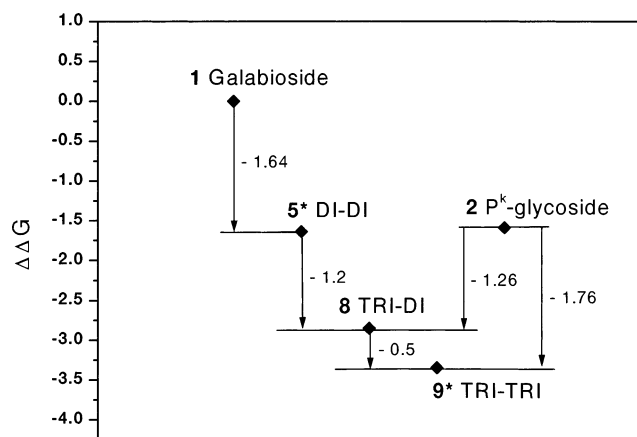(23) Jencks, W. P. *Proc. Natl. Acad. Sci. U.S.A.* **1981**, *78*, 4046–50.

Figure 4. Balance of the relative free energies of binding for a series of monovalent and bivalent ligands. The binding energy for galabioside **1** is taken as a reference. (∗) The $\Delta G°$ values for symmetrical compounds **5** and **9** are corrected by the statistical term $RT \ln 2$.

free energies presents compelling evidence that both binding sites 1 and 2 are simultaneously engaged in interaction with the bivalent ligands.

After establishing this fact, we turned our attention to the conformational analysis of bivalent ligands in order to find criteria that may facilitate a priori evaluation of different tethered structures. The relative activities of bivalent galabiosides **4**−**7**, in which the tether structures differ only by the central structural element, ethylene, propylene, phenylene, and squaric acid diamide, are used to evaluate this model.

The obvious advantage of Jencks' concept is the additivity of binding energies of individual interactions. However, with the exception of A−B ligands containing particularly rigid tethers, the interaction with a receptor will be a sequential rather than concerted process. In agreement with this generalization, it has been demonstrated that, for the case when two binding sites are engaged in an interaction with a tethered dimeric ligand, the increased binding constant results mainly from a decrease in the off-rate of the dimer.[24] Accordingly, the interaction of our dimeric ligands with two different P^k-binding sites of SLT-1 may be better represented by two distinct steps: binding first to one and then to another binding site (Scheme 3).

Obviously, the description of the system by Jencks' formula 1 may only be possible under a condition of overwhelming predominance of complete complex II among bound species. In this case, the observed binding constant is approximately the product of intermediate constants.

$$K_{app} \approx [II]/[L][R] = K_1 K_2 = K'_1 K'_2 \qquad (2)$$

As indicated by previously published NMR[16] and mass spectrometry data,[17] the difference between site 2 and site 1 affinities is at least an order of magnitude and no appreciable binding with site 1 occurs until a high degree of site 2 occupancy is achieved. Hence, for clarity, we may neglect the second route via I′ as 10 times less probable.

We assume that the binding constant of intermolecular interaction K_1 equals $2K_I$, where K_I is the binding constant of the monovalent binding of P^k-di- or trisaccharide to site 2. The intramolecular binding constant K_2 is directly proportional to the concentration of pendant ligand at the second binding site

(C_{local} is the "local" or "effective" concentration), and the corresponding intrinsic *monovalent* binding constant at the second site (K_{II}) as defined by the equation

$$K_2 = C_{local} K_{II} \qquad (3)$$

Empirical rules that allow estimation of C_{local} for the ends of polymeric tethers[6,25] are not applicable for short tethers of irregular structure. However, for a system with a relatively small number of atoms, a more straightforward approach can be taken to evaluate the radial density bias introduced by the conformational flexibility of the tether. The model we employ assumes that one ligand is bound in the protein site of highest affinity. This location or rather an atom of the immobilized ligand serves as a pivot or hinge point about which the second ligand and tether move. In our case, the position of the hinge atom O-2 of the β-Gal residue serves as the origin of internal coordinates. Molecular dynamics simulations are used to monitor the evolution of the system over a 5 ns time period.

The local concentration of the unbound tethered ligand in a volume circumscribed by two hemispheres with radii R and $R − \Delta R$ is given as

$$C_{local} = \frac{3 \times 10^{27} P(R,\Delta R)}{2\pi N_A (R^3 - (R - \Delta R)^3)}$$

$$= 792.73 \frac{P(R,\Delta R)}{(R^3 - (R - \Delta R)^3)} \qquad (4)$$

where R is the distance in Å between bound and unbound ligand; $P(R,\Delta R)$ is the probability that the pendant ligand is found between R and $R − \Delta R$ from the bound ligand; and N_A is Avogadro's number.

The radial probability function $P(R,\Delta R)$ may be obtained by analysis of the molecular dynamics simulation. For the dynamics analysis, the internal coordinate is naturally chosen to be the distance between the pivotal point, O-2 of the β-Gal of the bound galabiose, and the ring oxygen of β-Gal of the pendant galabiose, the latter being the closest to the center of gravity for this monosaccharide. Figure 5 shows how the radial concentrations of pendant ligands that are tethered by different linkers change with the distance.

At separation distance $R = 10.9$ Å, which corresponds to the distance of interest in the crystal structure, both ethylenediamine- and propylenediamine-based linkers appear to be substantially more favorable than the phenylenediamine-based tether, and the highest affinity is predicted for the squaric-acid-based tethered dimer. This tendency is in good agreement with the observed affinities for compounds **4**, **5**, **6**, and **7** (Table 1 and Figure 6). Evidently, the more subtle difference between homologues **4** and **5** is beyond the limitations of this method.

The difference in binding energies between univalent and bivalent P^k-trisaccharides **1** and **9** is 1.76 kcal/mol (see Figure 4), which corresponds to $K_2 = 20$ at ambient temperature. Taking into account the value of $C_{local} = 0.2$ M from the conformational analysis for the propylenediamine-based linker and solving eq 3 with respect to K_{II}, we can obtain the value 95 M^{-1} for the monovalent binding constant for the low affinity

(24) Kramer, R. H.; Karpen, J. W. *Nature* **1998**, *395*, 710−3.

(25) Gargano, J. M.; Ngo, T.; Kim, J. Y.; Acheson, D. W. K.; Lees, W. J. *J. Am. Chem. Soc.* **2001**, *123*, 12909−10.

Scheme 3
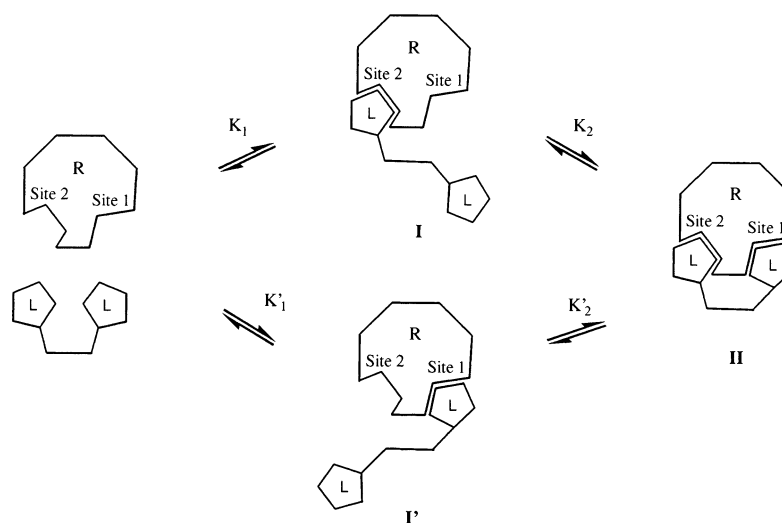
binding site 1. This is in good agreement with the magnitude of the low affinity binding constant, which was estimated to be 10−15% that of the dominant binding site, $K_a^I = 500-1000$ M^{-1}. This independent evaluation of the method also suggests that this approach can be used in the design of tethered multimeric ligands as one of the a priori selection criteria. This simple approach performs surprisingly well, considering that

Figure 5. Theoretical distribution of C_{local} for galabioside dimers **4**−**7** predicted on the basis of eq 4. The atom O-2′ belongs to the ligand held in site 2, while the atom O-5′ is part of the pendant ligand.

Figure 6. Correlation between experimental intramolecular binding constants K_2 for symmetrical dimers **4**−**7** and calculated local concentration of the pendant ligand at the low affinity binding site 1. (In the estimation of K_2, the statistical coefficient of 2 is taken into account.)

the estimate of the population of conformations capable of binding in the second site is based only on the radial distribution function for a single interatomic distance.

An advantage of this approach in distinguishing relatively small differences in activity of analogous bivalent ligands is that it does not depend on the evaluation of binding energies. It relies on estimation of the probability of supplementary interaction rather than its strength and indirectly takes into account all changes in conformational entropy (i.e., the sum of torsional entropies of single bonds in a tether) upon binding without actually calculating it. The magnitude of the radial distribution function at the binding site separation distance provides a convenient and computationally inexpensive means for approximating the local concentration of a pendant ligand at the secondary binding site for an arbitrary tether structure. It also reflects the radial nature of the ligand movements about the bound ligand. An alternative approach for evaluation of C_{local} involving calculation of the probability to find a pendant ligand in the vicinity of the binding site would require a large training set of bivalent ligands in order to define the capture distance, whereas the radial density distribution function permits direct comparison of any two ligands of interest.
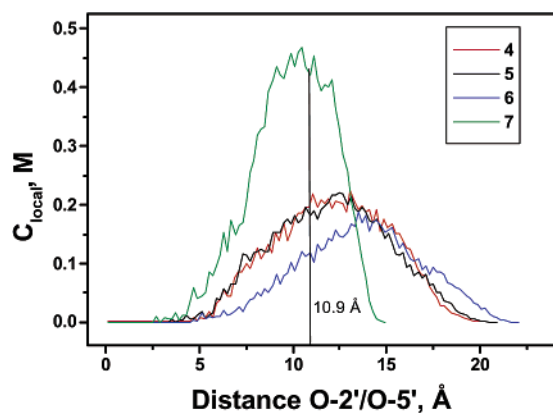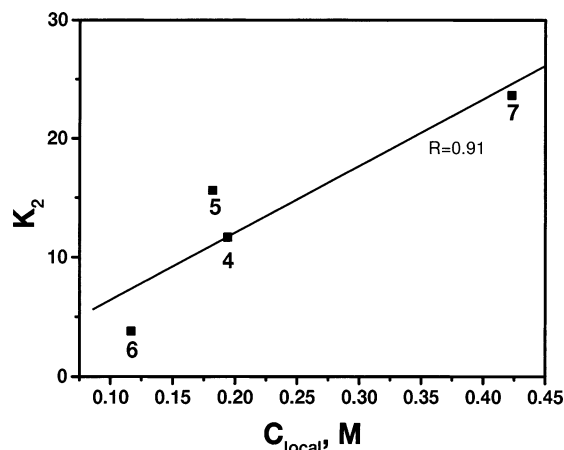
Conclusions

A predictive method to optimize tether length has been developed to facilitate the design of bivalent oligosaccharide ligands. MD simulations provide the local concentration of pendant ligands attached via a tether to one oligosaccharide that is locked in one sugar binding site. The tether length, at which the pendant ligand is most highly populated at the additional binding site, expressed as a radial distribution function is shown to correspond to optimal tether lengths determined experimentally. In addition, a simplified thermodynamic treatment provides the intrinsic affinities and binding energies for the intermolecular and intramolecular association events and permits the deconvolution of the contributions to the relative free binding energies for the set of bivalent ligands. We will show in a subsequent paper how this structure-based approach has been applied to tailoring larger architectures, which, starting from the original univalent ligand with millimolar activity, resulted in the design of a potent sub-nanomolar inhibitor.[5]

Experimental Section

General Methods. Optical rotations were measured on a Perkin-Elmer 241 polarimeter for samples in a 10 cm cell at ambient temperature (22 ± 2 °C). Analytical TLC was performed on silica gel 60-F_{254} (Merck) with detection by quenching of fluorescence and/or by charring with 10% H_2SO_4 in ethanol solution followed by heating at 180 °C. Column chromatography was performed on silica gel 60 (Merck, 40−60 μm), and solvents were distilled prior to use. Sep-Pak C_{18} cartridges (Waters) were conditioned prior to use by washing with methanol (10 mL) and water (20 mL). ^{1}H NMR spectra were recorded at 300 and 600 MHz (Varian) in $CDCl_3$ (referenced to residual $CHCl_3$ at δ_H 7.24 ppm), CD_3OD (referenced to residual CD_2HOD at δ_H 3.3 ppm), or in D_2O (referenced to external acetone at δ_H 2.225 ppm). First order *J* values are given in Hz. All commercial reagents were used as supplied; solvents were distilled from appropriate desiccants prior to use. After extraction, solutions in DCM were filtered through a cotton plug.

NMR Sample Preparation. The B_5 homopentamer of *Shiga*-like toxin was prepared in ^{15}N-enriched form as described.[16] A sample was prepared for NMR studies by dissolution of 2.5 mg of ^{15}N-enriched subunit in 250 μL of 100 mM phosphate buffer, pH 7.0, in a Shigemi 5 mm microcell. After acquisition of a ^{15}N−^{1}H HSQC spectrum of the protein, 2.3 mg of **9** in solid form was dissolved in the sample and a second ^{15}N−^{1}H HSQC spectrum was acquired under otherwise identical conditions to those of the first.

NMR Experiments. All spectra were acquired on a Varian Unity Inova 600 MHz spectrometer at a probe temperature of 303 K. Spectral widths of 5500 and 2400 Hz were utilized with 2048 and 256 complex points in the F2 and F1 dimensions, respectively. In total, 32 transients were acquired per t1 increment. Solvent suppression was achieved using the standard WATERGATE suppression scheme.[26]

Molecular Dynamics Simulations. All MD simulations were performed using Discover and the associated suite of software programs from Molecular Simulations Inc. (San Diego). The consistent valency force field (CVFF), without Morse and cross terms, was used with the effective dielectric constant set to 80. Each run consisted of 1 fs time step intervals for a total of 5 ns, with the temperature set to 1000 K. The resulting trajectories for each molecule were sampled every 250 fs, and the structural properties of interest evaluated as an average over 20 000 configurations.

The B_5 subunit−bivalent ligand complex was prepared from the coordinates of the crystal structure for SLT-1−P^k-trisaccharide (PDB entry 1BOS). One of the B subunits with complete trisaccharide occupancy of site 1 and site 2 was chosen. The positions for all atoms for side chains of amino acids numbers 13, 15, 16, 17, 19, 21, 28, 30, 32, 58, 60, 61, and 62 were retained, and the rest of the protein was deleted. The terminal glucose moiety was replaced by a methyl group, and the tether was constructed from standard fragments. Potentials were automatically assigned followed by manual correction, formal charges were set to 0, and partial charges for the ligand were automatically assigned, whereas for the protein atoms they were set to 0. The energy of the tether was minimized for 10 000 iterations using a conjugate gradient with fixed positions for the carbohydrates and protein prior to MD. The MD calculations were performed with fixed positions of the protein atoms and the positions of the bound methyl galabioside in site 2 tethered by a harmonic oscillator constrain force of 100 kcal/mol per atom.

Inhibition ELISA Assay. PVC microtiter plates (Gibco BRL Inc.) were incubated with *Shiga*-like toxin Type 1 (2.5 μg/mL, 100 μL/well) at room temperature overnight and then washed (6×) with PBST (0.05% Tween 20 in phosphate buffer saline, PBS). Blocking solution (2.5% skimmed milk in PBS, 100 μL/well) was added, and the plates were incubated for 1 h at room temperature and then washed (6×) with

(26) Sklenar, V.; Piotto, M.; Leppik, R.; Saudek, V. *J. Magn. Reson., Ser. A* **1993**, *102*, 241−5.

PBST. An inhibitor at decreasing concentrations (starting from ∼50 mg/mL, 3.16 dilution factor, 50 μL/well) was mixed with biotinylated P^k-BSA glycoconjugate (2 μg/mL, 50 μL/well), and the mixtures were applied to the plates in triplicate. After incubation at room temperature for 18 h, the plates were washed (6×) with PBST, incubated with streptavidin-horseradish peroxidase in PBST (1 μg/mL, 100 μL/well) for 1 h at room temperature, and then washed (6×) with PBST. 3,3′,5,5′-Tetramethylbenzidine (TMB) peroxidase substrate was added (both the streptavidin-horseradish peroxidase and its TMB substrate were purchased from Gibco BRL Inc.). After 2−5 min, the reaction was quenched by addition of H_3PO_4 (100 μL/well). The plates were read at 450 nm. Nonlinear data fitting into a logistic sigmoidal curve based on the Levenberg−Marquardt algorithm was performed using Microcal Origin 5.0 (Microcal Software, Inc., Northampton, MA 01060, USA).

Methyl 3,6-Di-*O*-benzyl-2-*O*-[2-(4-nitrophenoxycarbonyloxy)-ethyl]-4-*O*-(2,3,4,6-tetra-*O*-benzyl-α-D-galactopyranosyl)-β-D-galactopyranoside (11). To a solution of **10**[18] (490 mg, 0.521 mmol) in pyridine (3 mL) 4-nitrophenylchloroformate (158 mg, 1.5 equiv) was added. The mixture was stirred overnight at 40 °C, and then water (10 mL) was added. The mixture was diluted with DCM, washed with water, and the organic layer was concentrated. Chromatography of the residue on silica gel with pentane−ethyl acetate (85:15−75:25) gave **11** (542 mg, 94%), [α]$_D$ +40.7° (*c* 0.8; CHCl$_3$).^{1}H NMR (CDCl$_3$): δ 7.37−7.17 (m, 34 H, arom.), 5.04 (d, 1 H, $J_{1',2'}$ 2.0 Hz, H-1′), 4.89 (d, 1 H, ^2J 11.2 Hz, Bn), 4.88 (d, 1 H, ^2J 11.8 Hz, Bn), 4.80 (d, 1 H, ^2J 12.0 Hz, Bn), 4.73 (s, 2 H, Bn), 4.67 (d, 1 H, ^2J 11.8 Hz, Bn), 4.57 (d, 1 H, ^2J 12.9 Hz, Bn), 4.53 (d, 1 H, ^2J 11.3 Hz, Bn), 4.43−4.38 (m, 3 H, H-5′, CH$_2$), 4.27 (d, 1 H, ^2J 11.8 Hz, Bn), 4.22 (d, 1 H, ^2J 11.8 Hz, Bn), 4.19 (d, 1 H, $J_{1,2}$ 7.5 Hz, H-1), 4.14 (s, 2 H, Bn), 4.10−3.94 (m, 7 H, H-2′, H-3′, H-4′, H-4, H-6a, CH$_2$), 3.58−3.45 (m, 7 H, H-2, H-5, H-6b, H-6′a, Me), 3.35 (dd, 1 H, $J_{3,2}$ 9.9 Hz, $J_{3,4}$ 2.9 Hz, H-3), 3.26 (dd, 1 H, $J_{6'b,5'}$ 4.9 Hz, $J_{6'b,6'a}$ 8.4 Hz, H-6′b). Anal. Calcd. for C$_{64}$H$_{67}$NO$_{16}$: C, 69.49; H, 6.10; N, 1.27. Found: C, 69.52; H, 6.15; N, 1.29.

Methyl 3,6-Di-*O*-benzyl-2-*O*-(4-nitrophenoxycarbonyl)-4-*O*-(2,3,4,6-tetra-*O*-benzyl-α-D-galactopyranosyl)-β-D-galactopyranoside (13). To a solution of **12**[18] (393 mg, 0.438 mmol) in pyridine (3 mL) 4-nitrophenylchloroformate (106 mg, 1.2 equiv) was added. The mixture was stirred for 3 h at 50 °C, then diluted with DCM, washed with water, and concentrated. Chromatography of the residue on silica gel with pentane−ethyl acetate (80:20) gave **13** (396 mg, 85%), [α]$_D$ +38.1° (*c* 0.5; CHCl$_3$). ^{1}H NMR (CDCl$_3$): δ 7.32−7.01 (m, 34 H, arom.), 5.13 (dd, 1 H, $J_{2,1}$ 7.9 Hz, $J_{2,3}$ 10.3 Hz, H-2), 5.03 (broad s, 1 H, H-1′), 4.96−4.87 (m, 3 H, Bn), 4.74 (s, 2 H, Bn), 4.69 (d, 1 H, ^2J 11.8 Hz, Bn), 4.52 (d, 1 H, ^2J 11.1 Hz, Bn), 4.48−4.41 m, 3 H, H-5′, Bn), 4.28 (d, 1 H, ^2J 11.7 Hz, Bn), 4.21 (d, 1 H, ^2J 11.7 Hz, Bn), 4.18 (d, 1 H, $J_{4',3'}$ 2.7 Hz, H-4′), 4.14−3.98 (m, 6 H, H-1, H-4, H-6a, H-2′, H-3′, Bn), 3.61−3.50 (m, 7 H, H-3, H-5, H-6b, H-6′b, OMe), 3.17 (dd, 1 H, $J_{6'b,5'}$ 4.8 Hz, $J_{6'b,6'a}$ 8.6 Hz, H-6′b). Anal. Calcd. for C$_{62}$H$_{63}$NO$_{15}$: C, 70.11; H, 5.98; N, 1.32. Found: C, 70.08; H, 5.99; N, 1.32.

Methyl 4-*O*-[3,6-Di-*O*-benzyl-4-*O*-(2,3,4,6-tetra-*O*-benzyl-α-D-galactopyranosyl)-2-*O*-(2-hydroxyethyl)-β-D-galactopyranosyl]-2,3,6-tri-*O*-benzyl-β-D-glucopyranoside (15). To a solution of **14**[18] (570 mg, 0.411 mmol) and 4-methylmorpholine *N*-oxide (96 mg, 0.82 mmol) in an acetone−water (10 mL to 0.5 mL) mixture OsO$_4$ (0.5 mL, 0.1 g/mL solution in *t*-BuOH) was added. The mixture was stirred for 2 days then taken up in DCM, washed with water, and concentrated. To a solution of the residue in THF (15 mL) a solution of NaIO$_4$ (174 mg) in water (2 mL) was added. After stirring at 50 °C for 3 h, NaBH$_4$ (110 mg) was added and the suspension was stirred for 0.5 h, neutralized with AcOH, taken up in DCM, washed with water, and concentrated. Chromatography of the residue on silica gel in hexanes−ethyl acetate (70:30−65:35) gave **15** (490 mg, 87%), [α]$_D$ +36.1° (*c* 0.26; CHCl$_3$). ^{1}H NMR (CDCl$_3$): δ 7.4−7.1 (m, 45 H, arom.), 5.02−4.99 (m, 2 H, H-1″, Bn), 4.83−4.62 (m, 8 H, Bn), 4.50−4.32 (m, 6 H, H-1′, Bn), 4.28−4.09 (m, 7 H, H-1, H-4′, H-5″, Bn), 4.04 (dd, 1 H, $J_{2'',1''}$ 3.3 Hz, $J_{2'',3''}$ 10.3 Hz, H-2″), 4.02−3.70 (m, 8 H, H-4, H-6a, H-6b, H-5′, H-3″,

H-4″, CH$_2$), 3.52 (s, 3 H, Me), 3.62−3.35 (m, 7 H, H-3, H-5, H-2′, H-6′a, H-6″a, CH$_2$), 3.33 (dd, 1 H, $J_{2,1}$ 7.7 Hz, $J_{2,3}$ 9.0 Hz, H-2), 3.27−3.12 (m, 3H, H-3′, H-6′b, H-6″b). Anal. Calcd. for C$_{84}$H$_{92}$O$_{17}$: (1373.62) C, 73.45; H, 6.75. Found: C, 73.48; H, 6.74.

Methyl 4-*O*-[3,6-Di-*O*-benzyl-4-*O*-(2,3,4,6-tetra-*O*-benzyl-α-D-galactopyranosyl)-2-*O*-[2-(4-nitrophenyloxycarbonylethyl)ethyl]-β-D-galactopyranosyl]-2,3,6-tri-*O*-benzyl-β-D-glucopyranoside (16). A mixture of **15** (434 mg, 0.316 mmol) and 4-nitrophenylchloroformate (74 mg, 1.2 equiv) in dry pyridine (3 mL) was stirred for 4 h at 50 °C, and then the reaction was quenched with water, concentrated, and chromatographed on silica gel with pentane−ethyl acetate (80:20−75:25) to give **16** (406 mg, 85%), [α]$_D$ +29.0° (c 0.5; CHCl$_3$). ^{1}H NMR (CDCl$_3$): δ 8.17 (m, 2 H, arom.), 7.40−7.10 (m, 47 H, arom.), 5.02−5.00 (m, 2 H, H-1″, Bn), 4.85−4.62 (m, 8 H, Bn), 4.50−4.40 (m, 6 H, H-1′, Bn), 4.31−4.20 (m, 6 H, H-1, H-4′, CH$_2$, Bn), 4.15−3.82 (m, 12 H, H-4, H-6a, H-6b, H-5′, H-2″, H-3″, H-4″, H-5″, CH$_2$, Bn), 3.54 (t, 1 H, $J_{3,2}$ ≈ $J_{3,4}$ 9.0 Hz, H-3), 3.50 (s, 3 H, Me), 3.50−3.40 (m, 4 H, H-5, H-2′, H-6′a, H-6″a), 3.34 (dd, 1 H, $J_{2,1}$ 7.8 Hz, H-2), 3.29−3.20 (m, 2 H, H-6′b, H-6″b), 3.16 (dd, 1 H, $J_{3',2'}$ 8.4 Hz, $J_{3',4'}$ 4.7 Hz, H-3′). Anal. Calcd. for C$_{91}$H$_{95}$NO$_{21}$: C, 71.03; H, 6.22; N, 0.91. Found: C, 71.03; H, 6.29; N, 0.91.

Methyl 4-*O*-{2-*O*-[2-(3-Acetamidopropylaminocarbonyl)ethyl]-3,6-di-*O*-benzyl-4-*O*-(2,3,4,6-tetra-*O*-benzyl-α-D-galactopyranosyl)-β-D-galactopyranosyl}-2,3,6-tri-*O*-benzyl-β-D-glucopyranoside (17). A solution of **16** (64.5 mg, 42 μmol) in THF (2 mL) was added to a solution of 1,3-diaminopropane (15.5 mg, 210 μmol) in THF (0.5 mL). After 15 min, Ac$_2$O (0.3 mL) was added and the mixture was concentrated. Chromatography of the residue on silica gel with hexane−ethyl acetate (1:2) gave **17** (62.7 mg, 98%), [α]$_D$ +31.3° (c 0.2; CHCl$_3$). ^{1}H NMR (CDCl$_3$): δ 7.4−7.1 (m, 45 H, arom.), 6.14 (broad t, 1 H, NHAc), 5.80 (t, 1 H, ^3J 6.4 Hz, NH), 5.06−5.02 (m, 2 H, H-1″, Bn), 3.52 (s, 3 H, OMe), 4.86−3.26 (m, 41 H, H-1, H-2, H-3, H-4, H-5, H-6a, H-6b, H-1′, H-2′, H-4′, H-5′, H-6′a, H-6′b, H-2″, H-3″, H-4″, H-5″, H-6″a, H-6″b, Bn, OCH$_2$), 3.16−3.06 (m, 3 H, H-3′, C*H*$_2$NAc), 2.84−2.72 (m, 2 H, C*H*$_2$NCO$_2$), 1.92 (s, 3 H, Ac), 1.34−1.24 (m, 2 H, C*H*$_2$CH$_2$N). Anal. Calcd. for C$_{90}$H$_{102}$N$_2$O$_{19}$: C, 71.31; H, 6.78; N, 1.85. Found: C, 71.13; H, 6.82; N, 1.81.

N,N′-Bis{[methyl 3,6-di-*O*-benzyl-4-*O*-(2,3,4,6-tetra-*O*-benzyl-α-D-galactopyranosyl)-β-D-galactopyranoside-2-yloxy]ethyl}oxycarbonyl-ethylenediamine (18). A mixture of **13** (121 mg, 110 μmol) and ethylenediamine (3.3 mg, 55 μmol) in DMF (1 mL) was stirred for 1 h at 50 °C, then diluted with ethyl acetate (30 mL), washed with water, and concentrated. Chromatography of the residue on silica gel with pentane−ethyl acetate (1:1) gave **18** (87.6 mg, 80%), [α]$_D$ +37.4° (c 0.23; CHCl$_3$). ^{1}H NMR (CDCl$_3$): δ 7.36−7.16 (m, 60 H, arom.), 5.03 (s, 2 H, H-1′), 4.91−4.85 (m, 6 H, Bn, NH), 4.76 (d, 2 H, ^2J 12.5 Hz, Bn), 4.74 (s, 4 H, Bn), 4.66 (d, 2 H, ^2J 11.7 Hz, Bn), 4.66 (d, 2 H, ^2J 11.7 Hz, Bn), 4.58−4.51 (m, 4 H, Bn), 4.41−4.37 (m, 2 H, H-5′), 4.28−3.92 (m, 26 H, H-1, H-4, H-6a, H-2′, H-3′, H-4′, Bn, CH$_2$), 3.88−3.82 (m, 2 H, CH$_2$), 3.55−3.43 (m, 14 H, H-2, H-5, H-6b, H-6′a, OMe), 3.31 (dd, 2 H, $J_{3,2}$ 9.9 Hz, $J_{3,4}$ 2.8 Hz, H-3), 3.22 (dd, 2 H, $J_{6'b,5'}$ 4.9 Hz, $J_{6'b,6'a}$ 8.3 Hz, H-6′b), 3.10 (broad s, 4 H, CH$_2$N). Anal. Calcd. for C$_{118}$H$_{132}$N$_2$O$_{26}$: C, 71.07; H, 6.67; N, 1.40. Found: C, 70.89; H, 6.72; N, 1.42.

N,N′-Bis{[methyl 3,6-di-*O*-benzyl-4-*O*-(2,3,4,6-tetra-*O*-benzyl-α-D-galactopyranosyl)-β-D-galactopyranoside-2-yloxy]ethyl}oxycarbonyl-propylenediamine (19). Prepared as described for **18** from **13** (113 mg, 102 μmol) and 1,3-diaminopropane (3.78 mg, 51 μmol). Yield 100 mg (97%), [α]$_D$ +43.0° (c 0.33; CHCl$_3$). ^{1}H NMR (CDCl$_3$): δ 7.36−7.16 (m, 60 H, arom.), 5.00 (s, 2 H, H-1′), 4.92 (broad s, 2 H, NH), 4.86 (d, 2 H, ^2J 11.2 Hz, Bn), 4.83 (d, 2 H, ^2J 11.7 Hz, Bn), 4.73 (d, 2 H, ^2J 12.0 Hz, Bn), 4.72 (s, 4 H, Bn), 4.63 (d, 2 H, ^2J 11.9 Hz, Bn), 4.56−4.48 (m, 4 H, Bn), 4.38−4.34 (m, 2 H, H-5′), 4.26−3.78 (m, 28 H, H-1, H-4, H-6a, H-2′, H-3′, H-4′, Bn, CH$_2$O), 3.54−3.40 (m, 14 H, H-2, H-5, H-6b, H-6′a, OMe), 3.28 (dd, 2 H, $J_{3,2}$ 9.7 Hz, $J_{3,4}$ 2.4 Hz, H-3), 3.20 (dd, 2 H, $J_{6'b,5'}$ 5.1 Hz, $J_{6'b,6'a}$ 8.7 Hz, H-6′b), 3.04−

3.00 (m, 4 H, CH$_2$N), 1.48−1.39 (m, 2 H, CH$_2$). Anal. Calcd. for C$_{119}$H$_{134}$N$_2$O$_{26}$: C, 71.17; H, 6.72; N, 1.39. Found: C, 70.92; H, 6.61; N, 1.39.

N,N′-Bis{[methyl 3,6-di-*O*-benzyl-4-*O*-(2,3,4,6-tetra-*O*-benzyl-α-D-galactopyranosyl)-β-D-galactopyranoside-2-yloxy]ethyl}oxycarbonyl-(*p*-phenylenediamine) (20). A mixture of **11** (162 mg, 152 μmol), 1,4-phenylenediamine (8.2 mg, 76 μmol), and DMAP (20 mg) in DMF (2 mL) was stirred for 2 days at 50 °C, then diluted with ethyl acetate (30 mL), washed with water, and concentrated. Chromatography of the residue on silica gel with pentane−ethyl acetate (1:1) gave **20** (93 mg, 63%), [α]$_D$ +62.5° (c 0.3; CHCl$_3$). ^{1}H NMR (CDCl$_3$): δ 7.36−7.16 (m, 64 H, arom.), 6.38 (s, 2 H, NH), 5.19 (dd, 2 H, $J_{2,1}$ 8.0 Hz, $J_{2,3}$ 10.2 Hz, H-2), 5.03 (d, 2 H, $J_{1',2'}$ 3.2 Hz, H-1′), 4.94 (d, 2 H, ^2J 12.0 Hz, Bn), 4.88 (d, 2 H, ^2J 11.1 Hz, Bn), 4.79 (d, 2 H, ^2J 11.8 Hz, Bn), 4.77 (s, 4 H, Bn), 4.69 (d, 2 H, ^2J 11.8 Hz, Bn), 4.56−4.51 (m, 4 H, H-5′, Bn), 4.38−4.01 (m, 22 H, H-1, H-4, H-6a, H-2′, H-3′, H-4′, Bn), 3.58−3.53 (m, 6 H, H-5, H-6b, H-6′a), 3.50 (s, 6 H, OMe), 3.43 (dd, 2 H, $J_{3,4}$ 3.1 Hz, H-3), 3.21 (2 H, $J_{6'b,6'a}$ 8.9 Hz, H-6′b)). Anal. Calcd. for C$_{118}$H$_{124}$N$_2$O$_{24}$: C, 72.52; H, 6.40; N, 1.43. Found: C, 72.23; H, 6.44; N, 1.45.

N,N′-Bis{{methyl 4-*O*-[3,6-di-*O*-benzyl-4-*O*-(2,3,4,6-tetra-*O*-benzyl-α-D-galactopyranosyl)-β-D-galactopyranosyl]-2,3,6-tri-*O*-benzyl-β-D-glucopyranoside}-2′-yloxyethyl}oxycarbonyl-propylenediamine (21). To a solution of **16** (108 mg, 70 μmol) in THF (1.5 mL) 1,3-diaminopropane (2.6 mg, 35 μmol) was added. The mixture was stirred for 3 h at 50 °C, then concentrated, and chromatographed on silica gel with hexane−ethyl acetate (70:30−60:40) to give **21** (93 mg, 92.5%), [α]$_D$ +25.8° (c 0.25; CHCl$_3$). ^{1}H NMR (CDCl$_3$): δ 7.4−7.1 (m, 90 H, arom.), 5.53 (t, 2 H, ^3J 6.3 Hz, NH), 5.04−5.01 (m, 4 H, H-1″, Bn), 4.81 (d, 2 H, ^2J 11.2 Hz, Bn), 4.79 (d, 2 H, ^2J 11.1 Hz, Bn), 4.72−4.60 (m, 16 H, OCH$_2$, Bn), 4.49−4.24 (m, 22 H, H-1, H-1′, H-4′, Bn), 4.13−3.73 (m, 26 H, H-4, H-6a, H-6b, H-5′, H-6′a, H-2″, H-3″, H-4″, H-5″, OCH$_2$, Bn), 3.52 (t, 2 H, $J_{2,3}$ ≈ $J_{3,4}$ 9.0 Hz, H-3), 3.51 (s, 6 H, Me), 3.49−3.21 (m, 12 H, H-2, H-5, H-2′, H-6′b, H-6″a, H-6″b), 3.12 (dd, 2 H, $J_{3',2'}$ 8.2 Hz, $J_{3',4'}$ 4.7 Hz, H-3′), 2.75 (m, 4 H, CH$_2$N), 1.17 (t, 2 H, ^3J 6.2 Hz, C*H*$_2$CH$_2$N). Anal. Calcd. for C$_{173}$H$_{190}$N$_2$O$_{36}$: C, 72.31; H, 6.61; N, 0.97. Found: C, 72.32; H, 6.69; N, 0.96.

N-{[Methyl 3,6-di-*O*-benzyl-4-*O*-(2,3,4,6-tetra-*O*-benzyl-α-D-lactopyranosyl)-β-D-galactopyranoside-2-yloxy]ethyl}oxycarbonyl-N′-{{methyl 4-*O*-[3,6-di-*O*-benzyl-4-*O*-(2,3,4,6-tetra-*O*-benzyl-α-D-galactopyranosyl)-β-D-galactopyranosyl]-2,3,6-tri-*O*-benzyl-β-D-glucopyranoside}-2′-yloxyethyl}oxycarbonyl-propylenediamine (22). A solution of **16** (64.5 mg, 42 μmol) in THF (2 mL) was added to a solution of 1,3-diaminopropane (15.5 mg, 210 μmol) in THF (0.5 mL). After 15 min, the mixture was concentrated, taken up into ethyl acetate, washed with water, and concentrated. To a solution of the residue in THF (2 mL) a solution of **13** (50 mg, 45 μmol) was added. The mixture was incubated overnight at 40 °C and then concentrated. Chromatography of the residue on silica gel with hexane−ethyl acetate (1:1) gave **22** (93.7 mg, 90.8%), [α]$_D$ +34.3° (c 0.2; CHCl$_3$). ^{1}H NMR (CDCl$_3$): δ 7.4−7.1 (m, 75 H, arom.), 5.64 (t, 1 H, ^3J 6.3 Hz, (NH)^3), 5.05−5.00 (m, 3 H, H-(1″)^3, H-(1′)^2, Bn)^3), 4.89−3.70 (m, 53 H, H-1^3, H-4^3, H-(1′)^3, H-(3′)^3, H-(4′)^3, H-(5′)^3, H-(2″)^3, H-(3″)^3, H-(4″)^3, H-(5″)^3, H-1^2, H-4^2, H-(2′)^2, H-(3′)^2, H-(4′)^2, H-(5′)^2, Bn, CH$_2$O), 3.52 (s, 3 H, OMe), 3.49 (s, 3 H, OMe), 3.57−3.19 (m, 21 H, H-2^3, H-3^3, H-5^3, H-(2′)^3, H-(6′a)^3, H-(6′b)^3, H-(6″a)^3, H-(6″b)^3, H-2^2, H-3^2, H-(6a)^2, H-(6b)^2, H-5^2, H-(6′a)^2, H-(6′b)^2), 3.12 (dd, 2 H, $J_{3',2'}$ 8.2 Hz, $J_{3',4'}$ 4.7 Hz, H-3′), 3.13 (dd, 1 H, $J_{(3')3,(2')3}$ 8.25 Hz, $J_{(3')3, (4')3}$ 4.6 Hz, H-(3′)^3), 2.99−2.92 (m, 2 H, (CH$_2$N)^2), 2.82−2.73 (m, 2 H, (CH$_2$N)^3), 1.3−1.2 (m, 2 H, C*H*$_2$CH$_2$N). Anal. Calcd. for C$_{146}$H$_{162}$N$_2$O$_{31}$: C, 71.84; H, 6.69; N, 1.15. Found: C, 71.78; H, 6.61; N, 1.15.

Methyl 4-*O*-{2-*O*-[2-(3-Acetamidopropylaminocarbonyl)ethyl]-4-*O*-(α-D-galactopyranosyl)-β-D-galactopyranosyl}-β-D-glucopyranoside (3). The title compound was obtained in 89% yield by hydrogenation of **17** as described for the preparation of **4**, [α]$_D$ +46.4°

(*c* 0.3; H$_2$O). ^{1}H NMR (D$_2$O): δ 4.97 (d, 1 H, $J_{1'',2''}$ 3.7 Hz, H-1''), 4.53 (d, 1 H, $J_{1',2'}$ 7.8 Hz, H-1'), 4.38 (d, 1 H, $J_{1,2}$ 8.0 Hz, H-1), 4.35 (t, 1 H, $J_{5',6'a} \approx J_{5',6'b}$ 6.4 Hz, H-5''), 4.23–4.21 (m, 2 H, CH$_2$O), 4.10–3.57 (m, 16 H, H-3, H-4, H-5, H-6a, H-6b, H-3', H-4', H-5', H-6'a, H-6'b, H-3'', H-4'', H-6''a, H-6''b, CH$_2$O), 3.58 (s, 3 H, Me), 3.42 (dd, 1 H, $J_{2',3'}$ 9.9 Hz, H-2'), 3.30 (m, 1 H, H-2), 3.23–3.14 (m, 4 H, CH$_2$-CH$_2$CH$_2$N), 1.99 (s, 3 H, Ac), 1.76–1.66 (m, 2 H, CH_2CH$_3$N). ^{13}C NMR (D$_2$O): δ 174.88 (C=O), 159.24 (C=O), 103.92 (C-1β), 103.25 (C-1β), 101.27 (C-1α), 80.65, 78.67, 76.09, 75.88, 75.17, 73.76, 72.92, 72.15 (CH$_2$), 71.88, 69.98, 69.82, 69.37, 65.48 (CH$_2$), 61.46 (CH$_2$), 61.26 (CH$_2$), 60.79 (CH$_2$), 58.00 (CH$_3$), 38.68 (CH$_2$), 37.56 (CH$_2$), 29.17 (CH$_2$), 22.68 (CH$_3$). Electrospray ionization MS for C$_{27}$H$_{48}$N$_2$O$_{19}$Na: calcd 727.2749, found 727.2746.

***N*,*N*′-Bis{[methyl 4-*O*-(α-D-galactopyranosyl)-β-D-galactopyranoside-2-yloxy]ethyl}oxycarbonyl-ethylenediamine (4).** A mixture of **18** (78 mg, 39 μmol) and 10% Pd/C (30 mg) was suspended in AcOH (4 mL) and stirred overnight under hydrogen flow, then filtered, concentrated, dissolved in water, and applied to Sep-Pak (C-18). The cartridge was washed with water and then with 10% MeOH. Sugar containing fractions were concentrated to furnish **4** (30 mg, 84%), [α]$_D$ +84.5° (*c* 0.26; H$_2$O). ^{1}H NMR (D$_2$O): δ 4.98 (d, 2 H, $J_{1',2'}$ 3.8 Hz, H-1'), 4.42 (d, 2 H, $J_{1,2}$ 7.7 Hz, H-1), 4.35 (t, 2 H, $J_{5',6'a} \approx J_{5',6'b}$ = 6.4 Hz, H-5'), 4.25–4.18 (m, 4 H, CH$_2$O), 4.05 (d, 2 H, $J_{4,3}$ 3.1 Hz, H-4), 4.04 (d, 2 H, $J_{4',3'}$ 3.3 Hz, H-4'), 4.05–4.02 (m, 2 H, CH$_2$O), 3.94–3.89 (m, 6 H, H-6a, H-3', CH$_2$O), 3.86–3.83 (m, 4 H, H-6a, H-2'), 3.77 (dd, 2 H, $J_{3,2}$ 10.1 Hz, H-3), 3.75–3.69 (m, 6 H, H-5, H-6'a, H-6'b), 3.59 (s, 6 H, OMe), 3.48 (dd, 2 H, H-2), 3.26 (broad s, 4 H, CH$_2$N). ^{13}C NMR (D$_2$O): δ 159.23 (C=O), 104.62 (C-1β), 101.09 (C-1α), 80.61, 78.28, 75.74, 72.76, 71.86, 71.44 (CH$_2$), 70.02, 69.90, 69.54, 65.47 (CH$_2$), 61.51 (CH$_2$), 61.05 (CH$_2$), 58.12 (CH$_3$), 41.07 (CH$_2$). Electrospray ionization MS for C$_{34}$H$_{60}$N$_2$O$_{26}$Na: calcd 935.3332, found 935.3338.

***N*,*N*′-Bis{[methyl 4-*O*-(α-D-galactopyranosyl)-β-D-galactopyranoside-2-yloxy]ethyl}oxycarbonyl-propylenediamine (5).** The title compound (31.2 mg, 78%) was prepared from **19** (87 mg, 43.3 μmol) as described for **4**, [α]$_D$ +78.6° (*c* 0.3; H$_2$O). ^{1}H NMR (D$_2$O): δ 4.97 (d, 2 H, $J_{1',2'}$ 3.8 Hz, H-1'), 4.42 (d, 2 H, $J_{1,2}$ 7.9 Hz, H-1), 4.35 (t, 2 H, $J_{5',6'a} \approx J_{5',6'b}$ 6.4 Hz, H-5'), 4.24–4.17 (m, 4 H, CH$_2$O), 4.04 (d, 2 H, $J_{4,3}$ 3.1 Hz, H-4), 4.03 (d, 2 H, $J_{4',3'}$ 3.3 Hz, H-4'), 4.04–4.01 (m, 2 H, CH$_2$O), 3.94–3.89 (m, 6 H, H-6a, H-3', CH$_2$O), 3.85–3.83 (m, 4 H, H-6a, H-2'), 3.76 (dd, 2 H, $J_{3,2}$ 10.3 Hz, H-3), 3.75–3.69 (m, 6 H, H-5, H-6'a, H-6'b), 3.57 (s, 6 H, OMe), 3.38 (dd, 2 H, H-2), 3.18 (t, 4 H, J 6.6 Hz, CH$_2$N), 175–170 (m, 2 H, NCH$_2$CH_2CH$_2$N). ^{13}C NMR (D$_2$O): δ 159.27 (C=O), 104.66 (C-1β), 101.13 (C-1α), 80.55, 78.27, 75.74, 72.75, 71.83, 71.49 (CH$_2$), 69.99, 69.88, 69.53, 65.36 (CH$_2$), 61.46 (CH$_2$), 61.01 (CH$_2$), 58.08 (CH$_3$), 38.64 (CH$_2$). Electrospray ionization MS for C$_{35}$H$_{62}$N$_2$O$_{26}$Na: calcd 949.3488, found 949.3490.

***N*,*N*′-Bis{[methyl 4-*O*-(α-D-galactopyranosyl)-β-D-galactopyranoside-2-yloxy]ethyl}oxycarbonyl-(*p*-phenylenediamine) (6).** The title compound **6** (28.6 mg, 78%) was prepared from **20** (82.1 mg, 42 μmol) as described for **4**. Fractions with 20% MeOH were collected from Sep-Pak chromatography, [α]$_D$ +84.4° (*c* 0.34; H$_2$O). ^{1}H NMR (D$_2$O): δ 7.48 (s, 4H, arom.), 4.99 (d, 2 H, $J_{1',2'}$ 4.0 Hz, H-1'), 4.81 (dd, 2 H, $J_{2,1}$ 7.9 Hz, $J_{2,3}$ 9.9 Hz, H-2), 4.61 (d, 2 H, H-1), 4.39 (t, 2 H, $J_{5',6'a} \approx J_{5',6'b}$ 6.4 Hz, H-5'), 4.11 (d, 2 H, $J_{4,3}$ 2.9 Hz, H-4), 4.06 (d, 2 H, $J_{4',3'}$ 3.5 Hz, H-4'), 3.99–3.97 (m, 4 H, H-3, H-3'), 3.95 (dd, 2 H, $J_{6a,5}$ 7.3 Hz, $J_{6a,6b}$ 11.5 Hz, H-6a), 3.89–3.85 (m, 4 H, H-6b, H-2'), 3.82 (broad t, H-5), 3.72 (dd, 2 H, $J_{6'a,5'}$ 6.0 Hz, $J_{6'a,6'b}$ 11.5 Hz, H-6'a), 3.68 (dd, 2 H, $J_{6'b,5'}$ 6.9 Hz, H-6'b), 3.56 (s, 6 H, OMe). ^{13}C NMR (D$_2$O): δ 156.39 (C=O), 134.61 (arom.), 122.01 (arom.), 103.02 (C-1β), 101.47 (C-1α), 78.73, 76.10, 74.27, 71.82, 71.76, 71.74, 71.72, 71.67, 70.07, 70.01, 70.00, 69.92, 69.65, 61.47 (CH$_2$), 61.08 (CH$_2$), 58.18 (CH$_3$). Electrospray ionization MS for C$_{34}$H$_{52}$N$_2$O$_{24}$Na: calcd 895.2807, found 895.2813.

***N*-{[Methyl 4-*O*-(α-D-galactopyranosyl)-β-D-galactopyranoside-2-yloxy]ethyl}oxycarbonyl-*N*′-{{methyl 4-*O*-[4-*O*-(α-D-galactopy-**

ranosyl)-β-D-galactopyranosyl]-β-D-glucopyranoside}-2′-yloxyethyl}-oxycarbonyl-propylenediamine (8).** The per-benzyl ether **21** (91 mg, 37.3 μmol) was hydrogenated in AcOH in the presence of Pd/C (10%, 20 mg) for 24 h. The catalyst was filtered out. Supernatant was concentrated. The residue was passed through a Sep-Pak (C-18) cartridge in 10% MeOH to yield **8** (34.4 mg, 85%), [α]$_D$ +63.8° (*c* 0.4; H$_2$O). ^{1}H NMR (D$_2$O): δ 4.99 (m, 2 H, H-(1'')^3, H-(1')^2), 4.54 (d, 1 H, $J_{1',2'}$ 7.7 Hz, H-(1')^3), 4.43 (d, 1H, $J_{1,2}$ 7.7 Hz, H-1^2), 4.39 (d, 1 H, $J_{1,2}$ 8.0 Hz, H-1^3), 4.35 (t, 2 H, $J_{5',6''} \approx J_{5'',6''} \approx J_{5'',6''a} \approx J_{5'',6'b}$ 6.6 Hz, H-(5'')^3, H-(5')^2), 4.25–4.20 (m, 4 H, CH$_2$O), 4.10–3.56 (m, 28 H, H-3^3, H-4^3, H-5^3, H-(6a)^3, H-(6b)^3, H-(3')^3, H-(4')^3, H-(5')^3, H-(6'a)^3, H-(6'b)^3, H-(3'')^3, H-(4'')^3, H-(6''a)^3, H-(6''b)^3, H-3^2, H-4^2, H-5^2, H-(6a)^2, H-(6b)^2, H-(2')^2, H-(3')^2, H-(4')^2, H-(6'a)^2, H-(6'b)^2, CH$_2$O), 3.58 (s, 6 H, Me), 3.43 (dd, 1 H, $J_{2',3'}$ 9.9 Hz, H-(2')^3), 3.38 (dd, 1 H, $J_{2,3}$ 10.1 Hz, H-2^2), 3.31 (m, 1 H, H-2^3), 3.19 (broad t, 4 H, ^3J 6.7 Hz, CH$_2$N), 1.72 (m, 2 H, CH_2CH$_3$N). ^{13}C NMR (D$_2$O): δ 159.12 (C=O), 104.64 (C-1β), 103.90 (C-1β), 103.22 (C-1β), 101.25 (C-1α), 101.11 (C-1α), 80.67, 80.58, 78.70, 78.30, 76.11, 75.91, 75.75, 75.19, 73.78, 72.97, 72.78, 72.20 (CH$_2$), 71.91, 71.86, 71.51 (CH$_2$), 70.02, 69.91, 69.55, 69.40, 65.51 (CH$_2$), 65.40 (CH$_2$), 61.52 (CH$_2$), 61.30 (CH$_2$), 61.06 (CH$_2$), 60.84 (CH$_2$), 58.14 (CH$_3$), 58.06 (CH$_3$), 38.72 (CH$_2$), 29.89 (CH$_2$). Electrospray ionization MS for C$_{41}$H$_{72}$N$_2$O$_{31}$Na: calcd 1111.4016, found 1111.4002.

***N*,*N*′-Bis{{methyl 4-*O*-[4-*O*-(α-D-galactopyranosyl)-β-D-galacto-pyranosyl]-β-D-glucopyranoside}-2′-yloxyethyl}oxycarbonyl-propyl-enediamine (9).** The per-benzyl derivative **22** (83 mg, 28.9 μmol) was hydrogenated in AcOH in the presence of Pd/C (10%, 20 mg) for 24 h. The catalyst was filtered out, and the supernatant was concentrated. The residue was passed through a Sep-Pak (C-18) cartridge in 10% MeOH to yield **9** (29.3 mg, 81%), [α]$_D$ +51.7° (*c* 0.2; H$_2$O). ^{1}H NMR (D$_2$O): δ 4.97 (d, 2 H, $J_{1'',2''}$ 3.7 Hz, H-1''), 4.53 (d, 2 H, $J_{1',2'}$ 7.8 Hz, H-1'), 4.39 (d, 2 H, $J_{1,2}$ 8.0 Hz, H-1), 4.35 (t, 2 H, $J_{5'',6''a} \approx J_{5'',6'b}$ 6.6 Hz, H-5''), 4.23–4.21 (m, 4 H, CH$_2$O), 4.10–3.57 (m, 34 H, H-3, H-4, H-5, H-6a, H-6b, H-3', H-4', H-5', H-6'a, H-6'b, H-2'', H-3'', H-4'', H-6''a, H-6''b, CH$_2$O), 3.58 (s, 6 H, Me), 3.43 (dd, 2 H, $J_{2',3'}$ 10.1 Hz, H-2'), 3.30 (m, 2 H, H-2), 3.18 (t, 4 H, ^3J 6.7 Hz, CH$_2$N), 1.72 (m, 2 H, CH_2CH$_2$N). ^{13}C NMR (D$_2$O): δ 159.11 (C=O), 103.89 (C-1β), 103.22 (C-1β), 101.24 (C-1α), 80.67, 78.69, 76.19, 75.90, 75.27, 73.78, 72.96, 71.91 (CH$_2$), 70.00, 69.85, 69.39, 65.56 (CH$_2$), 61.52 (CH$_2$), 61.30 (CH$_2$), 60.84 (CH$_2$), 58.06 (CH$_3$), 38.78 (CH$_2$), 29.92 (CH$_2$). Electrospray ionization MS for C$_{47}$H$_{82}$N$_2$O$_{36}$Na: calcd 1273.4545, found 1273.4535.

Methyl 3,6-Di-*O*-benzyl-4-*O*-(2,3,4,6-tetra-*O*-benzyl-α-D-galactopyranosyl)-2-*O*-(2-methylsulfonyloxyethyl)-β-D-galactopyranoside (23). To a solution of **10**[18] (920 mg, 0.98 mmol) in Py (5 mL) MsCl (1.5 equiv) was added. After the reaction was stirred for 2 h at 0–15 °C, it was quenched with water, and the mixture was taken up into DCM, washed with water, and concentrated. Chromatography of the residue on silica gel in hexane–ethyl acetate (8:2–6:4) gave **23** (976 mg, 98%), [α]$_D$ +39.1° (*c* 1.0; CHCl$_3$). ^{1}H NMR (CDCl$_3$): δ 7.4–7.1 (m, 30 H, arom.), 5.03 (d, 1 H, $J_{1',2'}$ 2.1 Hz, H-1'), 4.91 (d, 1 H, ^2J 11.1 Hz, Bn), 4.88 (d, 1 H, ^2J 11.4 Hz, Bn), 4.78 (d, 1 H, ^2J 11.5 Hz, Bn), 4.67 (d, 1 H, ^2J 11.8 Hz, Bn), 4.76 (s, 2 H, Bn), 4.54 (d, 1 H, ^2J 11.2 Hz, Bn), 4.52 (d, 1 H, ^2J 12.7 Hz, Bn), 4.38 (dd, 1 H, $J_{5',6'a}$ 5.0 Hz, $J_{5',6'b}$ 8.6 Hz, H-5'), 4.29–4.20 (m, 4 H, Bn, CH$_2$OMs), 4.14 (d, 1 H, $J_{1,2}$ 7.5 Hz, H-1), 4.14 (s, 2 H, Bn), 4.09 (m, 3 H, H-4', H-2', H-3'), 4.04–3.91 (m, 4 H, H-4, H-6a, CH$_2$), 3.56–3.44 (m, 4 H, H-2, H-5, H-6b, H-6'a), 3.52 (s, 3 H, Me), 3.31 (dd, 1 H, $J_{3,4}$ 2.9 Hz, $J_{3,2}$ 9.9 Hz, H-3), 3.26 (dd, 1 H, $J_{6'b,6'a}$ 8.4 Hz, H-6'b), 2.88 (s, 3 H, Ms). Anal. Calcd. for C$_{58}$H$_{66}$O$_{14}$S: C, 68.35; H, 6.53; S, 3.15. Found: C, 68.30; H, 6.59; S, 3.30.

Methyl 3,6-Di-*O*-benzyl-4-*O*-(2,3,4,6-tetra-*O*-benzyl-α-D-galactopyranosyl)-2-*O*-(2-azidoethyl)-β-D-galactopyranoside (24). A suspension of **23** (510 mg, 0.5 mmol), NaN$_3$ (163 mg, 2.5 mmol), and cat. Bu$_4$NI (10 mg) in dry DMF (5 mL) was stirred for 3 h at 50 °C. The mixture was diluted with ethyl acetate, washed with brine, and

concentrated. Chromatography on silica gel with hexanes−ethyl acetate (8:1) gave azid **24** (393 mg, 81%), $[\alpha]_D$ +32.4° (*c* 0.4; CHCl₃). ¹H NMR (CDCl₃): δ 7.4−7.1 (m, 30 H, arom.), 5.02 (d, 1 H, $J_{1',2'}$ 1 Hz, H-1′), 4.90 (d, 1 H, ^2J 11.2 Hz, Bn), 4.86 (d, 1 H, ^2J 11.4 Hz, Bn), 4.78 (d, 1 H, ^2J 11.5 Hz, Bn), 4.76 (s, 2 H, Bn), 4.67 (d, 1 H, ^2J 11.8 Hz, Bn), 4.55 (d, 1 H, ^2J 11.2 Hz, Bn), 4.54 (d, 1 H, ^2J 12.7 Hz, Bn), 4.39 (dd, 1 H, $J_{5',6'a}$ 5.0 Hz, $J_{5',6'b}$ 8.6 Hz, H-5′), 4.26 (d, 1 H, ^2J 11.9 Hz, Bn), 4.22 (d, 1 H, ^2J 11.9 Hz, Bn), 4.16 (d, 1 H, $J_{1,2}$ 7.5 Hz, H-1), 4.13 (s, 2 H, Bn), 4.09 (m, 3 H, H-4′, H-2′, H-3′), 4.00−3.81 (m, 6 H, H-4, H-6a, CH₂), 3.56−3.44 (m, 3 H, H-2, H-5, H-6′a), 3.54 (s, 3 H, Me), 3.34−3.28 (m, 2 H, H-3, H-6b), 3.26 (dd, 1 H, $J_{6'b,6'a}$ 8.4 Hz, $J_{5',6'b}$ 4.8 Hz, H-6′b). Anal. Calcd. for C₅₇H₆₃N₃O₁₁: C, 70.86; H, 6.57; N, 4.35. Found: C, 71.04; H, 6.71; N, 4.35.

Methyl 4-*O*-(α-D-Galactopyranosyl)-2-*O*-(2-aminoethyl)-β-D-ga-lactopyranoside Acetic Acid Salt (25). Hydrogen gas was passed through a suspension of **24** (363 mg, 0.378 mmol) and Pd(OH)₂ (100 mg) in acetic acid (5 mL) for 24 h. The catalyst was filtered out, and the solution was concentrated to give yellow oil **25** (159 mg, 91%).¹H NMR (D₂O): δ 4.98 (d, 1 H, $J_{1',2'}$ 3.7 Hz, H-1′), 4.48 (d, 1 H, $J_{1,2}$ 7.7 Hz, H-1), 4.34 (t, 1 H, $J_{5',6'a} = J_{5',6'b}$ 6.1 Hz, H-5′), 4.10−4.01 (m, 9 H, H-4, H-4′, CH₂O), 3.97−3.70 (m, H, H-3, H-5, H-6a, H-6b, H-2′, H-3′, H-6′a, H-6′b, CH₂), 3.54 (s, 3 H, Me), 3.37 (dd, 1 H, $J_{2,3}$ 7.8 Hz, H-2), 3.22 (t, 2 H, ^3J 4.8 Hz, CH₂N). Electrospray ionization MS for C₁₅H₃₀NO₁₁: calcd 400.1819, found 400.1820

3,4-Di-{[methyl 4-*O*-(α-D-galactopyranosyl)-β-D-galactopyrano-side-2-yloxy]ethylamino}-3-cyclobutene-1,2-dion (7). To a solution of **25** (38 mg, 82 μmol) and 3,4-diethoxy-3-cyclobutene-1,2-dion (6.8 mg, 40 μmol) in MeOH Et₃N (~60 μL) was added. The mixture was stirred for 24 h, then concentrated, and chromatographed on silica gel with DCM−MeOH−water (8:2:0−500:500:5) to give title compound (35 mg, 85%), $[\alpha]_D$ +82.1° (*c* 0.6; H₂O). ¹H NMR (D₂O): δ 4.98 (d, 2 H, $J_{1',2'}$ 3.8 Hz, H-1′), 4.39 (d, 2 H, $J_{1,2}$ 7.7 Hz, H-1), 4.33 (t, 2 H, $J_{5',6'a} \approx J_{5',6'b}$ = 6.6 Hz, H-5′), 4.04−4.10 (m, 2 H, H-4, H-4′), 3.99−3.70 (m, H, H-3, H-5, H-6a, H-6b, H-2′, H-3′, H-6′a, H-6′b, CH₂), 3.54 (s, 6 H, OMe), 3.36 (dd, 2 H, $J_{2,3}$ 10.0 Hz, H-2).), ¹³C NMR (D₂O): δ 181.93 (C=C), 168.75 (C=O), 104.00 (C-1β), 100.48 (C-1α), 79.87, 77.80, 75.11, 72.34, 71.79 (CH₂), 71.31, 69.39, 69.31, 68.91, 60.95 (CH₂), 60.43 (CH₂), 57.35 (CH₃), 44.50 (CH₂). Electrospray ionization MS for C₃₄H₅₇N₂O₂₄: calcd 877.3301, found 877.3303.